Modelling of Fixed Bed Adsorption of Ciprofloxacin on $ZnCl_2$-Activated Carbon Derived from *Typha australis* Grass

A. B. Makama*[1], M. A. Sadiq †[2], and S. A. Saidu ‡[3]

[1]Department of Chemical Engineering Technology, The Federal Polytechnic, Nasarawa, Nigeria

[2]Department of Science Laboratory Technology, The Federal Polytechnic, Nasarawa, Nigeria

[3]Department of Chemistry, Federal University, Gashua, Nigeria

ABSTRACT

Fixed-bed adsorption has emerged as a widely employed industrial application in wastewater treatment processes. Various low-cost adsorbents have been stud- ied for their applicability in treating wastewater. In this study, the potential of $ZnCl_2$-activated carbon (TAAC) from Typha australis grass was investigated for ciprofloxacin (CIP) removal from synthetic wastewater in a fixed-bed adsorption column. The effect of flow rate (0.5 - 2.0 mL/min), bed height (5 - 10 cm), and initial drug concentration (25 - 100 mg/l) on the behavior of breakthrough curves was explained. Breakthrough time decreased with increasing flow rate and inlet CIP concentration but increased with increasing adsorbent bed height. Breakthrough curve analysis showed that CIP adsorption onto the TAAC material was most effective at a flow rate of 0.5 mL/min, inlet CIP concentration of 25 mg/L, and at a bed height of 10 cm. The maximum adsorption capacity of TAAC and removal efficiency were found to be 8.2 mg/g and 59.3%, respectively. Four common fixed-bed models were fitted to the breakthrough curves, and the Yan model displayed the best fit to the experimental data ($R^2 > 0.98$) across all conditions. These findings suggest that TAAC, a low-cost material, has the potential to be a promising adsorbent for the sustainable removal of CIP from water. However, further testing with surface modifications and real wastewater samples containing competitive anions is necessary to validate the performance of TAAC for practical applications.

Keywords— adsorption, activated carbon, ciprofloxacin, fixed-bed, typha grass

*abmakama@hotmail.com; Corresponding author
†faseediq06@gmail.com
‡saidusa1961@gmail.com

INTRODUCTION

Ciprofloxacin (CIP) is a widely used broad-spectrum antibiotic crucial in treating various bacterial infections[1]. However, its prevalence in the environment, particularly in water sources, has become a growing concern. Antibiotic enters ecosystems through multiple pathways, including manufacturing processes, consumer misuse, excretion, and improper disposal methods[2]. Numerous studies have detected CIP in wastewater and

freshwater sources globally, including in Nigeria[3, 4], highlighting the widespread nature of this contamination.

The environmental impact of ciprofloxacin extends beyond mere contamination. Its presence in water bodies contributes significantly to the emergence and proliferation of antibiotic-resistant (AR) pathogens[5]. This phenomenon poses a severe threat to public health, as it renders previously effective antibiotics ineffective against certain bacterial strains[6]. The implications of antibiotic resistance are severe and multifaceted. Infections caused by resistant bacteria become increasingly difficult to treat, often requiring more expensive, toxic, or less effective alternative antibiotics[7, 8]. This can result in prolonged illnesses, increased mortality rates, and extended hospital stays. Moreover, the economic burden of AR is substantial, encompassing higher healthcare costs, the need for more expensive drugs, and potential productivity losses due to prolonged illnesses[9, 10].

Given these serious implications, the removal of ciprofloxacin from water sources has become a critical environmental and public health priority. One promising approach to addressing this issue is the use of activated carbon for ciprofloxacin adsorption. Activated carbon (AC) is a highly porous material with an exceptional capacity to adsorb organic compounds[11], including antibiotics like ciprofloxacin[12]. The adsorption process involves the attachment of pollutant molecules to the surface of the activated carbon, effectively removing them from the water matrix[1, 13].

The efficacy of activated carbon in ciprofloxacin removal has been demonstrated through various research studies. These studies have explored the use of activated carbon derived from diverse sources, including: (i) graphene hydrogel[13], (ii) carbon nanotubes[14], (iii) *Prosopis juliflora*[15], and (iv) pumpkin seeds[5]. Each of these sources has shown promising results in the efficient elimination of ciprofloxacin from water, highlighting the versatility and potential of activated carbon as a treatment method.

The current study aims to build upon this existing body of research by investigating the adsorption of ciprofloxacin, an emerging contaminant, in a fixed-bed system packed with $ZnCl_2$-activated carbon from *Typha australis* grass[16]. The effects of flow rate, bed height, and initial CIP concentration were evaluated for the process. Four kinetic models – Bohart-Adams, Clark, Yan, and Yoon-Nelson – were applied to analyze adsorption kinetics, providing insights into adsorption rates, capacities, and

breakthrough times. By utilizing these models, the study aims to provide a detailed characterization of the adsorption process, offering insights into the efficiency and capacity of the activated carbon for antibiotic removal. This research contributes to the ongoing efforts to develop effective and sustainable methods for removing antibiotics from water sources using low-cost biomass adsorbent material, addressing a critical environmental and public health challenge.

MATERIALS AND METHODS

Materials

Chemicals and Reagents

Analytical-grade hydrochloric acid and sodium hydroxide which were sourced from Honeywell Research Chemicals distributors in Nigeria. Ciprofloxacin hydrochloride, in the form of Ciprotab USP 500 mg, was acquired from an authorized pharmacy in Nasarawa State, Nigeria. The molecular formula of ciprofloxacin hydrochloride monohydrate is $C_{17}H_{18}FN_3O_3HCl \cdot H_2O$, and its chemical structure is depicted in creffig:zwitterionic-ciprofloxacin (a). Double-distilled water was used to prepare all solutions in the study.

$ZnCl_2$-Activated Carbon

Typha australis grass $ZnCl_2$-activated carbon produced and characterized in our earlier work[16] was used as the adsorbent material. Some properties of the *T. australis*- activated carbon (TAAC) are given in Table 1.

Table 1: Characteristics of *T. australis* $ZnCl_2$-activated carbon. Data from Makama et al.(Makama et al., 2024)[16]

Parameter	Value
Powder size	37 µm
Specific surface area (SBET, N2)	424.5 $m^2\ g^{-1}$
pH_{PZC}	6.6
Density	410 $kg\ m^{-3}$
Vmicro	0.164 $cm^3\ g^{-1}$
Vmeso	0.074 $cm^3\ g^{-1}$
Pore size, DP	2.65 nm

Zwitterionic Ciprofloxacin

Ciprofloxacin (CIP) is a zwitterionic compound with two pKa values at pK_{a1} = 6.1 and pK_{a2} = 8.7. The predominant form of CIP varies

depending on the pH of the environment. It is primarily cationic at pH <6.1, mainly zwitterionic at pH between 6.1 to 8.7, and predominantly anionic at pH >8.7. Figure Fig. 1(b) illustrates this pH-dependent speciation of CIP. At the study's working pH of 7.0, the zwitterionic form of CIP ($CIP^{\pm}$) is the dominant species, accounting for approximately 87.6% of the total CIP present, as reported by Rodríguez López et al. (2021)[17].

Artificial Ciprofloxacin Wastewater

The preparation of ciprofloxacin solutions for the study involved two main steps. First, a 1000 mg/L stock solution was created by crushing two Ciprotab USP 500 mg tablets into a fine powder, dissolving it in double-distilled (DD) water in a 1 L volumetric flask, and adjusting the volume to exactly 1 liter[18]. This stock solution was then refrigerated for later use. In the second step, artificial $CIP^{\pm}$-laden wastewater was prepared by diluting the

stock solution to create working solutions at concentrations of 25 mg/L, 50 mg/L, and 100 mg/L using DD-water. The pH of each working solution was carefully adjusted to 7.0 ± 0.2 using HCl and NaOH, with a pH meter.

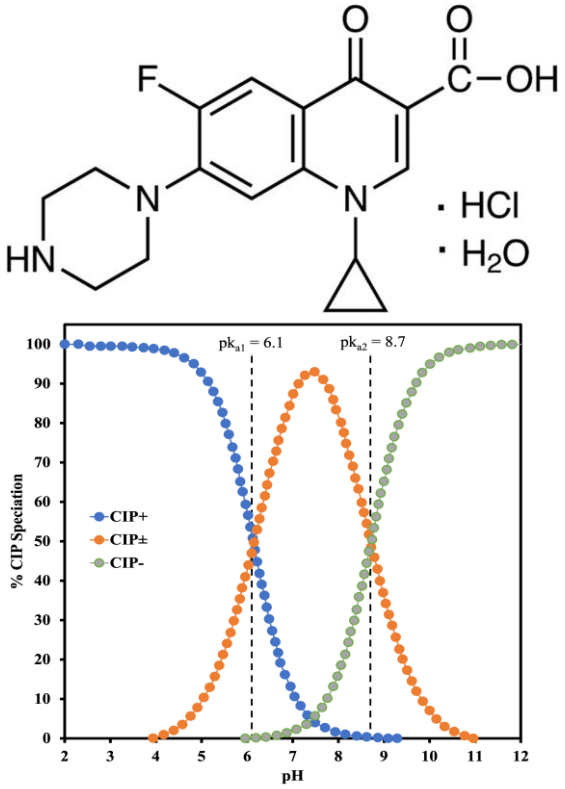

(a) **(b)**

Figure 1: (a) Chemical structure of ciprofloxacin hydrochloride monohydrate (Aphora Research

Inc., 2007) and (b) distribution of CIP species as a function of pH. Adapted from Makama et al. (2020)[42].

Fixed-Bed Adsorption Procedure

The fixed-bed sorption experiments were performed using a Pyrex glass column with a length of 300 mm, an internal diameter of 10 mm, and a volume of 4712.39 mm^3 (calculated using the formula $\pi r^2 h$). The column was filled with a specific quantity of adsorbent material to achieve the desired bed heights and capped at both ends with wire mesh and glass wool. This setup[19] prevented the loss of adsorbent material, avoiding changes in bed height and ensuring proper liquid distribution (as illustrated in Fig. 2). The experiments were conducted under varying conditions: bed heights ranging from 5 to 10 cm, inlet flow rates between 1 and 3 mL/min, and inlet antibiotic concentrations from 25 to 100 mg/L. The pH was maintained at 7.0 with minimal variation (less than 0.2) during the operation.

Prior to starting the experiments, DD-water was pumped upwards through the packed col- umn until a stable flow was established and left overnight to ensure a closely packed arrangement of particles with no void, channels, or cracks. Subsequently, the CIP test solution was introduced into the column using a peristaltic pump (Masterflex) at a controlled flow rate. Breakthrough curves were generated by collecting outflow samples at 30-minute intervals. The tests were per- formed at room temperature (30.0 ± 1.5) ˚C. Residual CIP concentrations were measured using ultraviolet-visible (UV-vis) spectrophotometry (mini 1240, Shimadzu) at a wavelength of 276 nm.

Theory and Column Data Analysis

Theory

The effectiveness of adsorbent and the dynamic behavior of a fixed-bed column can be assessed through the analysis of breakthrough curves[20]. These curves illustrate the loading behavior of CIP in wastewater treatment using fixed-bed operations. Typically, breakthrough curves plot the adsorbed pollutant concentration (C_{ads}) or normalized concentration (C_t/C_0) against the volume of effluent or time for a specific bed height[20]. In this work, the breakthrough point (t_b) is defined as the time in which the output concentration reaches 10% of the initial concentration (C_t/C_0 = 0.10) and the exhaustion (saturation) point (t_e) as the time at which the C_t/C_0 remains virtually constant.

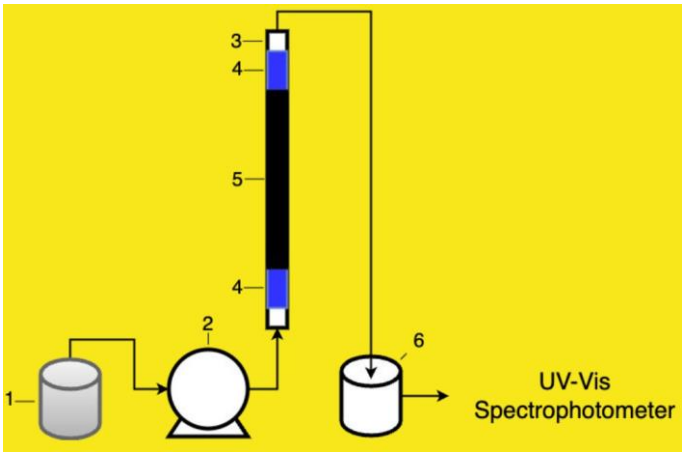

Figure 2: Experimental setup. 1. Artificial CIP wastewater, 2. Peristaltic Pump, 3. Adsorp- tion Column, 4. Ceramic Beads, 5. *TL*-PAC, and 6. Effluent Collector.

From the breakthrough curve, several key fixed-bed design parameters that provide valuable insights into the efficiency and performance of the fixed-bed adsorption process for CIP removal from wastewater can be derived [12, 19, 21, 22] including:

1. The volume of effluent (V_{eff} in mL) is given by

$$V_{\text{eff}} = Q \times t_{\infty} \tag{1}$$

where t_{∞} is the total flow time in min.

2. The empty bed contact time (EBCT in min) is obtained using

$$\text{EBCT} = \frac{\text{EBV}}{Q} \tag{2}$$

where EBV is the empty bed volume (mL); Q is the flow rate (mL/min); m is the mass of TAAC (g).

3. Total amount of CIP pollutant fed to the column (m_{tot} in mg): Determined using the equation

$$m_{\text{tot}} = \frac{Q \cdot C_0 \cdot t_{\infty}}{1000} \tag{3}$$

4. Total amount of CIP retained in the column (q_{tot} in mg) calculated from the area under the breakthrough curve (AUBC) using Eq. (4).

$$\begin{aligned} q_{\text{tot}} &= Q \int_{t_0}^{t_e} C_{\text{ads}} dt \\ &= Q \cdot C_0 \int_{t_0}^{t_e} \left(1 - \frac{C_t}{C_0}\right) dt \end{aligned} \tag{4}$$

where $C_{\text{ads}} = C_0 - C_t$.

5. Total CIP % removal efficiency (i.e. the column performance, E) is calculated as

$$E = \frac{q_{\text{tot}}}{m_{\text{tot}}} \times 100 \tag{5}$$

6. Column adsorption capacity (q_e in mg/g) at saturation is expressed as

$$\begin{aligned} q_e &= \frac{q_{\text{tot}}}{m} \\ &= \frac{Q \cdot C_0}{m} \int_{t_0}^{t_e} \left(1 - \frac{C_t}{C_0}\right) dt \end{aligned} \tag{6}$$

7. Column adsorption capacity (q_b in mg/g) at breakthrough is expressed as

$$q_b = \frac{Q \cdot C_0}{m} \int_{t_0}^{t_b} \left(1 - \frac{C_t}{C_0}\right) dt \tag{7}$$

8. The fractional bed utilization (FBU) is

$$\text{FBU} = \frac{q_b}{q_e} \tag{8}$$

9. Height of mass transfer zone(h_{MTZ}) is

$$\begin{aligned} h_{\text{MTZ}} &= Z(1 - \text{FBU}) \\ &= \left(1 - \frac{q_b}{q_e}\right) Z \\ &= \left(1 - \frac{t_b}{t_e}\right) Z \end{aligned} \tag{9}$$

10. Carbon utilization rate :

$$\text{CUR} = \frac{m}{Q \cdot t_e} \tag{10}$$

11. Throughput (TP)

$$\begin{aligned} \text{TP} &= \frac{1}{\text{CUR}} \\ &= \frac{Q \cdot t_e}{m} \end{aligned} \tag{11}$$

Mathematical Modelling

Several mathematical models [19, 20] have been formulated to elucidate the characteristics of column adsorption experiments conducted in laboratory settings. In this study, four distinct adsorption models, namely the Bohart-Adams [23, 24, 25, 26] models were employed to characterised the adsorption of CIP on the TAAC. The non- linear form of these models as described by [27] are presented in Eqs. (12) and(15).

Bohart-Adams Model: The Adams-Bohart model is a widely used model for describing the initial part of the breakthrough curve in fixed-bed adsorption processes. This model is based on the fundamental assumption that the rate of adsorption is directly proportional to both the concentration of the adsorbing species and the remaining adsorption capacity of the adsorbent[23]. The mathematical expression of the

Adams-Bohart model is given by Eq.(12).

$$\frac{C_t}{C_0} = \exp\left(k_{BA} \cdot C_0 \cdot t - k_{BA} \cdot N_0 \cdot \frac{h_b}{U}\right) \quad (12)$$

where C_0 is inlet CIP concentration in mg/L; C_t is effluent CIP concentration at time t in mg/L; C_t/C_0 is the dimensionless adsorbate concentration (ratio of effluent to influent concentration); h_b is column bed height in cm; and k_{BA} is the Adams–Bohart kinetic rate constant in L/(mg min). N_0 is saturation concentration (i.e the adsorption capacity per unit volume) of CIP in mg/L; U is linear velocity. It is calculated by dividing inlet flow rate, Q (cm^3/min) by the column cross sectional area, A (cm^2) of the bed ($U = Q/A$) in cm/min; and t is run time in minutes.

Clark Model The Clark model is a mathematical model used to describe the adsorption of pollutants in a fixed-bed adsorber. It combines the concepts of mass transfer and adsorption isotherms, specifically the Freundlich isotherm, to provide a more comprehensive understand- ing of the adsorption process. Key assumptions of the Clark model[25] : (i) The adsorption rate is proportional to both the concentration of the adsorbate in the fluid phase and the remaining adsorption capacity of the adsorbent. The adsorption equilibrium follows the Freundlich isotherm., and (ii) Axial dispersion and external mass transfer resistances are negligible. The mathematical expression of the Clark model is given by:

$$\frac{C_t}{C_0} = \frac{1}{1 + \left(\frac{t \cdot C_0}{q_0 \cdot V}\right)^{1/n}} \quad (13)$$

where: q_0 is the initial adsorption capacity (mg/g), V is the total volume of the liquid phase (L), and n is the Freundlich exponent (dimensionless).

Yan Model The Yan model is another fixed-bed adsorption model that is commonly used to describe the breakthrough behavior in fixed-bed adsorption processes. This model is based on these three assumptions[24] : (i) The adsorption rate is proportional to both the concentration of the adsorbate in the fluid phase and the remaining adsorption capacity of the adsorbent. (ii) The adsorption equilibrium follows the Langmuir isotherm., and (iii) Axial dispersion and external mass transfer resistances are negligible, The mathematical expression of the Yan model is given by:

$$\frac{C_t}{C_0} = \frac{1}{1 + \exp(k_Y(\frac{q_Y \cdot C_0 \cdot t}{m} - t))} \quad (14)$$

Where k_Y is the Yan kinetic constant (L/mg·min), q_Y is the maximum adsorption capacity (mg/g). All other terms are remain as previously defined above.

***Yoon-Nelson Model*:** The Yoon-Nelson model (YNM) is a relatively straightforward and attractive option among the various mathematical models used to describe fixed-bed adsorption processes. Unlike some of the other more complex models, the Yoon-Nelson model is based on a simple and intuitive assumption. The fundamental premise of the YNM is that the rate of decrease in the adsorption probability for an adsorbate molecule is directly proportional to the probability of adsorption of the adsorbate and the probability of the adsorbent bed breakthrough[28]. The YNM is specifically applicable to single-component adsorption systems[29]. The nonlinear equation that describes the Yoon-Nelson model is as follows:

$$\frac{C_t}{C_0} = \frac{1}{1 + e^{k_{YN} \cdot (t - \tau)}} \quad (15)$$

where k_{YN} = is Yoon–Nelson rate constant in 1/min and τ = is time required for 50% of the CIP to breakthrough in min. Other terms are as perviously defined in Eq. (12).

RESULTS AND DISCUSSIONS

Effects of Operational Parameters

To evaluate the effectiveness of TAAC as a $CIP^{\pm}$ adsorbent, the influence of inlet flow rate, bed height, and initial $CIP^{\pm}$ concentration on the process was examined. These factors are known to significantly impact adsorption performance of fixed-bed adsorption process[30]. The results of these tests are depicted in Figs. 3 to 5. The breakthrough curve shows a typical S-shape, indicating the gradual saturation of the adsorbent. This shape indi- cates non-ideal transport behavior in the adsorption process [20]. All results showed that complete saturation (C_t/C_0 = 1) was not achieved in any of the tested systems. This outcome aligns with previous observations in similar studies, including CIP adsorption on

different carbon materials[12, 31] and adsorption of other compounds on various adsorbents[13, 22, 32, 33, 34]. The incomplete saturation may be attributed to slower adsorption rates in certain parts of the column, potentially requiring extended periods to reach maximum saturation levels [19, 35].

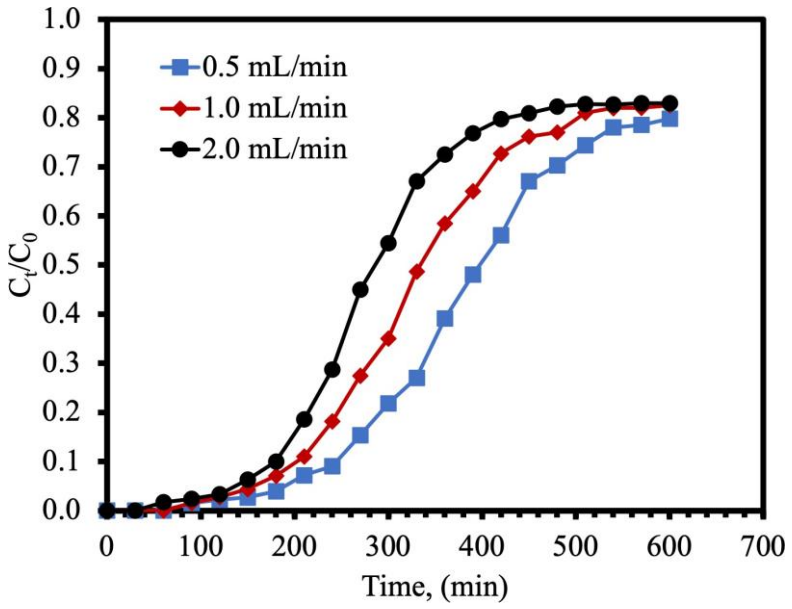

Figure 3: Effect of flow rate on breakthrough curve of CIP adsorption onto TAAC. *Conditions*: h_b: 100 mm, C_0: 50 mg/L, pH 7.0 ± 0.2.

Effect of Volumetric Flow rate

The impact of flow rates on CIP breakthrough curves is shown in Fig. 3. The experiments were conducted at three different volumetric flow rates of 0.5, 1.0, and 1.5 mL/min, while keeping inlet concentration (50 mg/L), bed height (100 mm), and pH (7.0 ± 0.2) constant. The profiles showed that higher flow rates led to earlier breakthrough times (t_b). Specifically, the t_bs were approximately 245.2, 202.3, and 180.0 min for flow rates of 0.5, 1.0, and 1.5 mL/min, respectively. Similarly, the exhaustion times decreased as the flow rate increased. This trend is explained by the longer contact time between CIP and TAAC at lower flow rates, allowing for more thorough interaction within the column. In contrast, higher flow rates reduce the contact time, limiting the efficiency of mass transfer between the contaminant and the adsorbent material [36, 37].

The analysis of the fixed-column operating parameters across different flow rates (Table 2) shows that the removal efficiency is highest at 0.5 mL/min (68.78%) and decreases with in- creasing flow rates. While the

adsorption capacity at exhaustion is higher at 2.0 mL/min, this comes at the cost of lower removal efficiency, faster breakthrough, and exhaustion times, as well as reduced carbon utilization. The mass transfer zone (MTZ) increases with higher flow rates, indicating greater mass transfer resistance (Fernández-Andrade et al., 2022) limiting CIP adsorption. Accordingly, the overall efficiency of the operation is best at 0.5 mL/min. This flow rate maximizes removal efficiency, prolongs breakthrough and exhaustion times, and opti- mizes carbon utilization, making it the most effective flow rate for maintaining a high-quality operation with minimal maintenance and resource usage. Thus, 0.5 ml/min was selected to evaluate the effects of bed height (h_b) and inlet concentration (C_0). Similar observations have been reported in the literature by [31] and [12] for fixed-column adsorption of CIP onto granular activated carbon.

Table 2: Operation conditions and estimated breakthrough adsorption parameters for CIP removal from artificial wastewater in fixed bed column using TAAC as adsorbent. Conditions: pH = 7.0 ± 0.2 and temperature = (30.0 ± 1.5) ˚C.

Operating Conditions							
Q (mL/min)	0.5	1.0	2.0	0.5	0.5	0.5	0.5
C_0 (mg/L)	50.0	50.0	50.0	50.0	50.0	25	100
Z (mm)	100	100	100	50	70	100	100
Adsorption Parameters							
EBV (mL)	7.85	7.85	7.85	3.93	5.5	7.85	7.85
EBCT (min)	15.7	7.9	3.9	7.9	11	15.7	15.7
t_∞, (min)	600	600	600	600	600	600	600
t_e (min)	540	510	480	480	510	540	420
V_∞ (mL)	300	600	1200	300	300	300	300
m_{tot} (mg)	15	30	60	15	15	7.5	30
q_{tot} (mg)	8	13.7	26.3	8.2	7	4.5	13.6
E (%)	68.78	45.60	43.80	54.50	46.50	59.3	45.2
q_e (mg/g)	2.50	4.20	8.20	5.10	3.10	1.4	4.2
t_b (min)	245.20	202.31	180.00	156.16	112.50	269.7	163.0
q_b (mg/g)	0.11	0.21	0.39	0.07	0.04	0.07	0.11
FBU	0.44	0.51	0.48	0.14	0.13	0.536	0.26
h_{MTZ} (mm)	54.60	60.30	62.50	33.70	54.60	35	42.8
CUR (g/L)	11.93	6.31	3.35	13.42	12.63	11.93	15.33
TP (L/g)	0.08	0.16	0.30	0.07	0.08	0.08	0.07

Effect of Adsorbent Bed Height

The impact of adsorbent bed height on breakthrough curve of CIP/TAAC fixed-bed system is shown in Fig. 4. The study was conducted at three different bed heights of 5, 7, and 10 cm while keeping C_0 (100 mg/L), Q (0.5 mL/min), and pH (7.0 ± 0.2) constant. Increasing bed height from 50 mm to

100 mm results in longer breakthrough and exhaustion times [31]. For example, t_b increases from 156.16 min at 50 mm to 245.20 min at 100 mm as shown in Table 2. A taller bed height provides more adsorbent material, which prolongs the time before saturation is reached [39]. Similarly, higher bed heights generally improve removal efficiency (from 54.50% at 50 mm to 68.78% at 100 mm), as there is more TAAC available to capture the CIP. The column adsorption capacity at breakthrough also increases with bed height, reflecting the greater amount of adsorbate retained within the column as the bed height increases. However, it's important to note that the total amount of CIP adsorbed increases with bed height, the adsorption capacity (q_e) decreases.

Similar observation has been reported by [30] and he attributed it more CIP molecules compared to available adsorption sites. These observations regarding the effect of bed height on breakthrough curves align with findings of [31, 40] in their studies of fixed-bed adsorption of antibiotics on activated carbon and graphene oxide, respectively.

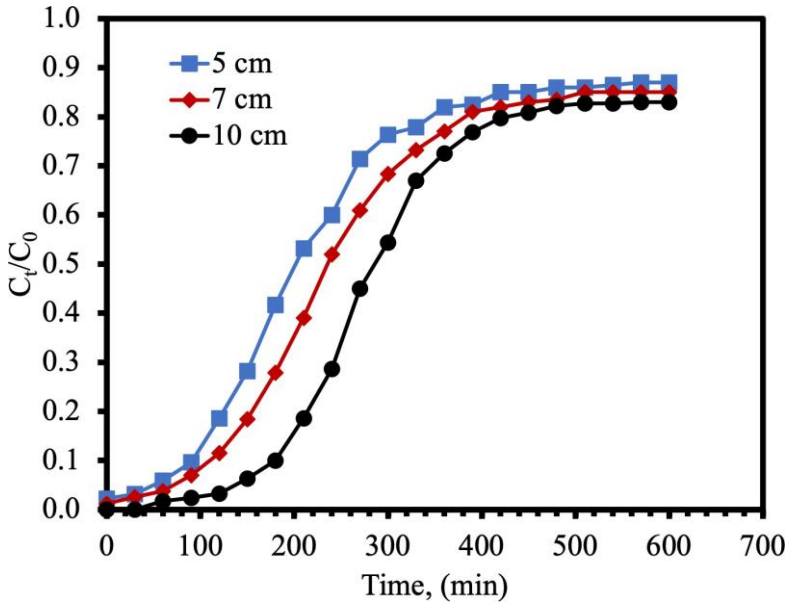

Figure 4: Effect of bed height on breakthrough curve of CIP adsorption onto TAAC. *Conditions*: Q: 2 mL/min, C_0: 50 mg/L, and pH: 7.0 ± 0.2.

Effect of inlet CIP Concentration

The Effect of Inlet concentration of CIP on breakthrough curve is depicted in Fig. 5. it can be observed that with increase in C_0 (25 - 100 mg/L), the breakthrough curves exhibited a displacement towards the origin causing the breakthrough times (t_b) decreased with increasing C_0 from 269.7 min at 25 mg/L to 163.0 min at 100 mg/L. Exhaustion time (t_e) is reached quickly in tests with higher concentrations; this may also be due to the rapid saturation of the available active sites of the TAAC [19]. The rapid saturation of the adsorbent bed can be attributed to the increased driving force for mass transfer in the adsorption process resulting from higher inlet concentrations. This behavior is related to enhancement of driving force for mass transfer across the liquid film along with acceleration of adsorption rate which leads to an early saturation of the fixed-bed [41]

Effect of inlet CIP Concentration

The Effect of Inlet concentration of CIP on breakthrough curve is depicted in Fig. 5. it can be observed that with increase in C_0 (25 - 100 mg/L), the breakthrough curves exhibited a displacement towards the origin causing the breakthrough times (t_b) decreased with increasing C_0 from 269.7 min at 25 mg/L to 163.0 min at 100 mg/L. Exhaustion time (t_e) is reached quickly in tests with higher concentrations; this may also be due to the rapid saturation of the available active sites of the TAAC[19]. The rapid saturation of the adsorbent bed

can be attributed to the increased driving force for mass transfer in the adsorption process resulting from higher inlet concentrations. This behavior is related to enhancement of driving force for mass transfer across the liquid film along with acceleration of adsorption rate which leads to an early saturation of the fixed-bed [41].

Kinetics Modeling of Fixed-Bed Adsorption Data

Mathematical modeling is fundamental to the design, scale-up and successful operation of a real world fixed-bed adsorption column. Towards this goal, the Bohart-Adams, Clark, Yan, and Yoon-Nelson models described in Section 2.3.2 were fitted to the breakthrough curves ob- tained experimentally (Fig. 6). Table 3 presents the parameters of the models adjusted to the experimental data.

The computed parameters show that as the flow rate increases from 0.5 to 2.0 mL/min, the Bohart-Adams model shows a slight increase in k_{BA}, while N_0 increases significantly. In the Clark model, the parameter A decreases, and r shows a slight increase. For the Yan model, q decreases as a increases. Meanwhile, the Yoon-Nelson model indicates a slight increase in

kYN, accompanied by a decrease in τ. These trends suggest that higher flow rates accelerate adsorption kinetics but result in shorter breakthrough times. The unexpected increase in N0 for the Bohart-Adams model, indicating higher adsorption capacity at higher flowrates, may warrant further investigation.

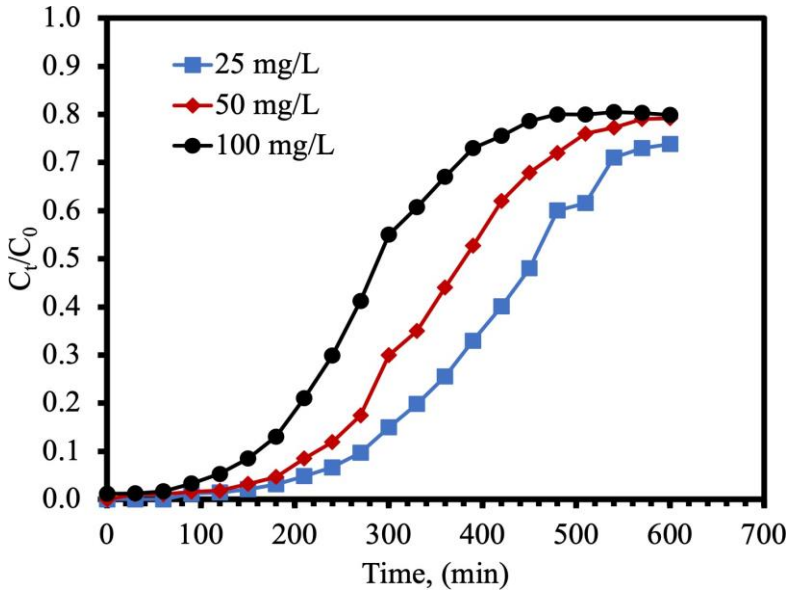

Figure 5: Effect of inlet concentration on breakthrough curve of $CIP^{\pm}$ adsorption onto TAAC.

Conditions: flow rate, 2 mL/min; initial CIP concentration 50 mg/L; pH 7.0 ± 0.2.

Table 3: Conditions and model parameters of breakthrough curves for the CIP-TAAC system

Operating Conditions							
Q (mL/min)	0.5	1.0	2.0	0.5	0.5	0.5	0.5
C_0 (mg/L)	50.0	50.0	50.0	50.0	50.0	25	100
Z (mm)	100	100	100	50	70	100	100
Bohart-Adams							
k_{BA} (L/mg·min) 10^{-4}	2.2	2.26	2.47	2.18	2.2	4.04	1.04
N_0 (mg/L)	1029.1	1600.1	3055.4	1567.8	925.6	580.2	1581.7
R^2	0.9837	0.9719	0.9504	0.9628	0.9556	0.9871	0.9434
Clark							
A	357.32	191.35	141.83	95.09	47.99	454.81	78.26
r (1/min)	0.0128	0.0131	0.0143	0.0126	0.0127	0.0119	0.0119
R^2	0.9767	0.9631	0.9394	0.9527	0.9450	0.9811	0.9308
Yan							
qY (mg/g)	4.19	3.74	3.54	3.18	2.66	4.17	3.09
k_Y (L/mg·min) 10^{-3}	2.5	2.9	3.4	3.3	4.1	2.2	3.3
R^2	0.9944	0.9912	0.982	0.9892	0.9900	0.9934	0.9809
Yoon-Nelson							
k_{YN} (1/min)	0.011	0.0113	0.0123	0.0109	0.011	0.0101	0.0104
τ (min)	411.64	355.58	305.54	313.55	259.18	464.13	316.33
R^2	0.9837	0.9719	0.9504	0.9628	0.9556	0.9871	0.9434

Kinetics Modeling of Fixed-Bed Adsorption Data

Mathematical modeling is fundamental to the design, scale-up and successful operation of a real world fixed-bed adsorption column. Towards this goal, the Bohart-Adams, Clark, Yan, and Yoon-Nelson models described in Section 2.3.2 were fitted to the breakthrough curves ob- tained experimentally (Fig. 6). Table 3 presents the parameters of the models adjusted to the experimental data.

The computed parameters show that as the flow rate increases from 0.5 to 2.0 mL/min, the Bohart-Adams model shows a slight increase in k_{BA}, while N_0 increases significantly. In the Clark model, the parameter A decreases, and r shows a slight increase. For the Yan model, q decreases as a increases. Meanwhile, the Yoon-Nelson model indicates a slight increase in k_{YN}, accompanied by a decrease in τ. These trends suggest that higher flow rates accelerate adsorption kinetics but result in shorter breakthrough times. The unexpected increase in N_0 for the Bohart-Adams model, indicating higher adsorption capacity at higher flow rates, may warrant further investigation.

Regarding the effect of initial concentration (C_0), as C_0 increases from 25 to 100 mg/L, the Bohart-Adams model shows a decrease in k_{BA} and an increase in N_0. The Clark model sees a decrease in A, with r remaining

relatively stable. In the Yan model, *q* decreases while *a* increases. The Yoon-Nelson model shows k_{YN} remaining nearly constant as tau decreases. Higher initial concentrations lead to faster breakthrough times (lower τ) and generally reduced adsorption capacity, as indicated by the lower q values in the Yan model. The increase in N_0 for the Bohart-Adams model, suggesting higher capacity at elevated concentrations, aligns with expectations.

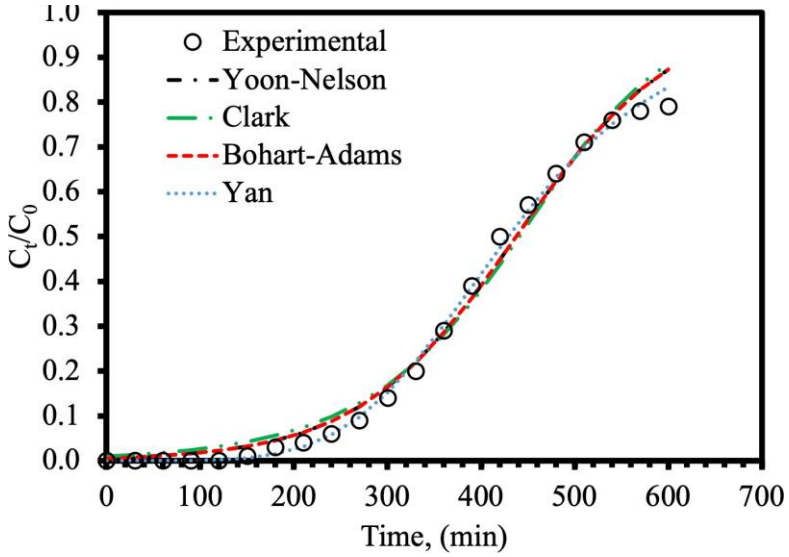

Figure 6: Experimental and predicted (using various models) breakthrough curves for CIP adsorption on TAAC. C_0 = 100 mg/L, H_b = 5.0 cm, Q_0 = 2.0 mL/min, and pH = 7.0 ± 0.2.

Analysis of bed height (Z) reveals that as Z decreases from 100 to 50 mm, the Bohart- Adams model maintains a relatively constant k_{BA}, while N_0 increases. The Clark model shows a decrease in *A*, with *r* remaining stable. The Yan model exhibits a decrease in q and an increase in a. Similarly, the Yoon-Nelson model shows a constant k_{YN} and a decrease in τ. These findings suggest that shorter bed heights result in quicker breakthroughs and generally reduced adsorption capacity, which is expected.

The model performance, based on R^2 values, indicates that the Yan model consistently outperforms the others across all conditions (R^2 > 0.98). The Bohart-Adams and Yoon-Nelson models show identical R^2 values, suggesting they may be mathematically equivalent for this system. The Clark model generally performs well, though slightly less effectively than the others.

CONCLUSION

The study evaluated $ZnCl_2$-activated carbon derived from *Typha australis*

(TAAC) as an ad- sorbent for removing ciprofloxacin (CIP) from aqueous solutions. The adsorption performance was influenced by several operational parameters, including inlet flow rate, bed height, and ini- tial CIP concentration. Higher flow rates resulted in earlier breakthrough times and reduced overall adsorption efficiency. Lower flow rates provided longer contact time between the CIP and TAAC, enhancing the interaction within the column and improving removal efficiency. In- creasing the bed height led to longer breakthrough and exhaustion times, indicating improved removal efficiency and higher total adsorption capacity. Higher initial concentrations of CIP led to faster breakthrough and exhaustion times due to the rapid saturation of the available active sites in the adsorbent. The maximum adsorption capacity of TAAC and removal efficiency were found to be 8.2 mg/g and 59.3%, respectively. The Yan model showed the best fit to the ex- perimental data, outperforming other models. Hence, this model can be used to describe the adsorption performance of CIP in a fixed-bed column. These findings suggest that TAAC, a low-cost material, has the potential to be a promising adsorbent for the sustainable removal of CIP from water. However, further testing with surface modifications and real wastewater samples containing competitive anions is necessary to validate the performance of TAAC for

practical applications.

ACKNOWLEDGEMENT

The researchers express their gratitude to the Tertiary Education Trust Fund (TETFund) for financially supporting this investigation through the Institutional Based Research (IBR) grant awarded.

REFERENCES

1. Bartolomé-Álvarez, J., & Solves-Ferriz, V. (2020). Increase in methicillin-resistant and ciprofloxacin-susceptible staphylococcus aureus in osteoarticular, skin and soft tis- sue infections. *Rev Esp Quimioter*, *33*(2), 143–144.

2. Larsson, D. G. J., & Flach, C.-F. (2022). Antibiotic resistance in the environment. *Nat. Rev. Microbiol.*, *20*(5), 257–269.

3. Ghosh, S., Pourebrahimi, S., Malloum, A., Ajala, O. J., AlKafaas, S. S., Onyeaka, H., Nnaji, N. D., Oroke, A., Bornman, C., Christian, O., Ahmadi, S., & Wani, M. Y. (2023). A review on ciprofloxacin removal from wastewater as a pharmaceutical con- taminant: Covering adsorption to advanced oxidation processes to computational studies. *Mater Today Commun*, *37*, 107500.

4. Wilkinson, J. L., Boxall, A. B. A.,

Kolpin, D. W., Leung, K. M. Y., Lai, R. W. S., Galbán- Malagón, C., Adell, A. D., Mondon, J., Metian, M., Marchant, R. A., Bouzas- Monroy, A., Cuni-Sanchez, A., Coors, A., Carriquiriborde, P., Rojo, M., Gordon, C., Cara, M., Moermond, M., Luarte, T., … Teta, C. (2022). Pharmaceutical pol- lution of the world's rivers. *Proc. Natl. Acad. Sci. USA*, *119*(8), e2113947119.

5. Alacabey, İ. (2022). Antibiotic removal from the aquatic environment with activated car- bon produced from pumpkin seeds. *Molecules*, *27*(4).

6. WHO. (2022). *The WHO AWaRe (Access, Watch, Reserve) antibiotic book* [Available at: https://apps.who.int/iris/bitstream/h andle/10665/365135/WHO-MHP-HPS-EML- 2022.02-eng.pdf]. World Health Organization.

7. Dadgostar, P. (2019). Antimicrobial resistance: Implications and costs. *Infect Drug Resist*, *12*, 3903–3910.

8. Friedman, N. D., Temkin, E., & Carmeli, Y. (2016). The negative impact of antibiotic resistance. *Clin Microbiol Infect*, *22*(5), 416–422.

9. Murray, C. J. L., Ikuta, K. S., Sharara, F., Swetschinski, L., Aguilar, G. R., Gray, A., Han, C., Bisignano, C., Rao, P., Wool, E., Johnson, S. C., Browne, A. J., Chipeta, M. G., Fell, F., Hackett, S., Haines-Woodhouse, G., Hamadani, B. H. K., Kumaran, E. A. P., McManigal, B., … Naghavi, M. (2022). Global burden of bacterial antimi- crobial resistance in 2019: A systematic analysis [Publisher: Elsevier]. *The Lancet*, *399*(10325), 629–655.

10. Poudel, A. N., Zhu, S., Cooper, N., Little, P., Tarrant, C., Hickman, M., & Yao, G. (2023). The economic burden of antibiotic resistance: A systematic review and meta-analysis. *PLoS One*, *18*(5), e0285170.

11. Soni, R., Bhardwaj, S., & Shukla, D. P. (2020). Various water-treatment technologies for inorganic contaminants: Current status and future aspects. In P. Devi, P. Singh, & S. K. Kansal (Editors), *Inorganic pollutants in water* (Pages 273–295). Elsevier.

12. Gupta, A., & Garg, A. (2019). Adsorption and oxidation of ciprofloxacin in a fixed bed column using activated sludge derived activated carbon. *J Environl Manage*.

13. Ma, J., Yang, M., Yu, F., & Zheng, J. (2015). Water-enhanced removal of ciprofloxacin from water by porous graphene hydrogel. *Sci Rep*, *5*(1), 13578.

14. Elamin, M. R., Abdulkhair, B. Y., & Elzupir, A. O. (2023). Removal of ciprofloxacin and indigo carmine from water by carbon nanotubes fabricated from a low-cost precursor: Solution parameters and recyclability. *Ain Shams Eng J*, *14*(1), 101844.

15. Chandrasekaran, A., Patra, C., Narayanasamy, S., & Subbiah, S. (2020). Adsorptive re- moval of ciprofloxacin and amoxicillin from single and binary aqueous systems using acid-activated carbon from prosopis juliflora. *Environ Res*, *188*, 109825.

16. Makama, A. B., Sadiq, M. A., & Saidu, S. A. (2024). Microwave-assisted synthesis of $zncl_2$-activated carbon from typha australis grass: Multi-response process optimisation and characterisation. *Nigerian J Technol Edu*, *23*(2), 128–144.

17. Rodríguez López, L., Cela-Dablanca, R., Núñez-Delgado, A., Álvarez-Rodríguez, E., Fernández- Calviño, D., & Arias-Estévez, M. (2021). Photodegradation of ciprofloxacin, clar- ithromycin and trimethoprim: Influence of ph and humic acids. *Molecules*, *26*, 3080.

18. Chen, J., Tomasek, M., & Gau, V. (2021). Categorizing microbial growth inhibition through quantification of 16s rrna growth marker with stripwells covering a spec- trum of antimicrobial conditions. *MethodsX*, *8*, 101453.

19. Antonelli, R., Malpass, G. R. P., da Silva, M. G. C., & Vieira, M. G. A. (2021). Fixed-bed adsorption of ciprofloxacin onto bentonite clay: Characterization, mathematical modeling, and DFT-based calculations. *Ind Eng Chem Res*, *60*(10), 4030–4040.

20. Patel, H. (2019). Fixed-bed column adsorption study: A comprehensive review. *Appl Wa- ter Sci*, *9*(3), 45.

21. Hanbali, Holail, H., & Hammud, H. (2014). Remediation of lead by pretreated red al- gae: Adsorption isotherm, kinetic, column modeling and simulation studies. *Green Chem Lett Rev*, *7* (4), 342–358.

22. Mekonnen, D. T., Alemayehu, E., & Lennartz, B. (2021). Fixed-bed column technique for the removal of phosphate from water using leftover coal. *Materials*, *14*(19).

23. Bohart, G. S., & Adams, E. Q. (1920). Some Aspects of the Behavior of Charcoal with Respect to Chlorine.1. *J Am Chem Soc*, *42*(3), 523–544 doi: 10.1021/ja01448a018.

24. Yan, G., & Viraraghavan, T. (2001). Heavy metal removal in a biosorption column by immobilized m. rouxii biomass. *Bioresour Technol*, *78*(3), 243–249.

25. Clark, R. M. (1987). Evaluating the cost and performance of field-scale granular activated carbon systems. *Environ Sci Technol*, *21*(6), 573–580.

26. Yoon, Y. H., & Nelson, J. H. (1984). Application of Gas Adsorption Kinetics. I. A The- oretical Model for Respirator Cartridge Service Life. *Am Ind Hyg Assoc J*, *45*(8), 509–516.

27. Abin-Bazaine, A. A., Olmos-Marquez, M. A., & Campos-Trujillo, A. (2024). A fixed-bed column sorption: Breakthrough curves modeling. In D. K. Margeta & D. A. Farkaš (Editors), *Sorption - new perspectives and applications*. IntechOpen.

28. Mani, S. K., & Bhandari, R. (2022). Efficient fluoride removal by a fixed-bed column of self-assembled zr(iv)-, fe(iii)-, cu(ii)-complexed polyvinyl alcohol hydrogel beads. *ACS Omega*, *7*(17), 15048–15063.

29. Lim, A. P., & Aris, A. Z. (2014). Continuous fixed-bed column study and adsorption modeling: Removal of cadmium (II) and lead (II) ions in aqueous solution by dead calcareous skeletons. *Biochem Eng J*, *87*, 50–61.

30. Chen, S., Yue, Q., Gao, B., Li, Q., Xu, X., & Fu, K. (2012). Adsorption of hexavalent chromium from aqueous solution by modified corn stalk: A fixed-bed column study [Special issue on the Challenges in Environmental Science and Engineering]. *Biore- sour Technol*, *113*, 114–120.

31. Darweesh, T. M., & Ahmed, M. J. (2017). Adsorption of ciprofloxacin and norfloxacin from aqueous solution onto granular activated carbon in

fixed bed column. *Ecotoxicol. Environ. Saf.*, *138*, 139–145.

32. Lima, L. F., de Andrade, J. R., da Silva, M. G. C., & Vieira, M. G. A. (2017). Fixed Bed Adsorption of Benzene, Toluene, and Xylene (BTX) Contaminants from Monocom- ponent and Multicomponent Solutions Using a Commercial Organoclay. *Ind Eng Chem Res*, *56*(21), 6326–6336.

33. Patel, H. (2020). Batch and continuous fixed bed adsorption of heavy metals removal using activated charcoal from neem (*Azadirachta indica*) leaf powder. *Sci Rep*, *10*(1), 16895.

34. Peñafiel, M. E., Matesanz, J. M., Vanegas, E., Bermejo, D., Mosteo, R., & Ormad, M. P. (2021). Comparative adsorption of ciprofloxacin on sugarcane bagasse from ecuador and on commercial powdered activated carbon. *Sci Total Environ*, *750*, 141498.

35. de Andrade, J. R., Oliveira, M. F., Canevesi, R. L. S., Landers, R., da Silva, M. G. C., & Vieira, M. G. A. (2020). Comparative adsorption of diclofenac sodium and losartan potassium in organophilic clay-packed fixed-bed: X-ray photoelectron spectroscopy characterization, experimental tests and theoretical study on DFT-based chemical descriptors. *J Mol Liq*, *312*, 113427.

36. Nidheesh, P. V., Gandhimathi, R., Ramesh, S. T., & Singh, T. S. A. (2012). Adsorption and desorption characteristics of crystal violet in bottom ash column. *J Urban Environ Eng*, *6*(1), 18–29.

37. Se-Il Yang, D.-K. C., Ju-Yong Park, & Kim, S.-H. (2009). Effects of the residence time in four-bed pressure swing adsorption process. *Separation Science and Technology*, *44*(5), 1023–1044.

38. Fernández-Andrade, K. J., González-Vargas, M. C., Rodríguez-Rico, I. L., Ruiz-Reyes,E., Quiroz-Fernández, L. S., Baquerizo-Crespo, R. J., & Rodríguez-Díaz, J. M. (2022).Evaluation of mass transfer in packed column for competitive adsorption of tartrazine and brilliant blue FCF: A statistical analysis. *Results Eng*, *14*, 100449.

39. Reynel-Avila, H. E., Mendoza-Castillo, D. I., Bonilla-Petriciolet, A., & Silvestre-Albero, J. (2015). Assessment of naproxen adsorption on bone char in aqueous solutions using batch and fixed-bed processes. *J Mol Liq*, *209*, 187–195.

40. Dong, S., Sun, Y., Wu, J., Wu, B., Creamer, A. E., & Gao, B. (2016). Graphene oxide as filter media to remove levofloxacin and lead from aqueous solution. *Chemosphere*, *150*, 759–764.

41. Gupta, S., & Babu, B. V. (2009). Modeling, simulation, and experimental validation for continuous cr(vi) removal from aqueous solutions using sawdust as an adsorbent. *Bioresour Technol*, *100*(23), 5633–5640.

42. Makama, A., Salmiaton, A., Choong, T., Hamid, M., Abdullah, N., & Saion, E. (2020). Influence of parameters and radical scavengers on the visible-light-induced degradation of ciprofloxacin in ZnO/SnS_2 nanocomposite suspension: Identification of transformation products. *Chemosphere*, *253*, 126689.